Development Of A Mathematical Model To Determine The Accuracy Of The Algorithm Of Shape From Polarization

Elena Smirnova, Evgenii Vikulov
«PolarMetr» LTD
Saint-Petersburg, Russia
elena.smirnova@polarmetr.com,
evgenii.vikulov@polarmetr.com

Viacheslav Gulvanskii
Saint Petersburg Electrotechnical University
Saint-Petersburg, Russia
vvgulvanskii@etu.ru

Michael Smirnov, Maria Mamaeva
Saint Petersburg University
Saint-Petersburg, Russia
m.n.smirnov@spbu.ru, st048842@student.spbu.ru

Abstract--**There are a large number of devices on market of 3D scanners that are able to get form of 3D surfaces of objects on different physical principles: laser lidars, systems with optical cameras, time-of-flight sensors and etc. At the moment, SONY company released sensors with polarizing spraying on the matrix, what in the aggregate with algorithm SFP – shape from polarization – can give information about the shape of the surface of the object, herewith without using active radiation sources. For creation of algorithms, creation of prototypes it is required to make modeling. Therefore, this article describes the process of creating a mathematical apparatus for processing polarized light data, based on the theory of micro-surface reflection of light. This mathematical apparatus will let to simulate the polarization of light depending on the location of the camera, the light and the inclination of the surface. A simulation and comparison with the results were made in the article.**

I. INTRODUCTION

Three-dimensional (3D) reconstruction is a key research topic in the field of computer vision, for which various approaches have been proposed. Fundamental research is based on basic physical parameters of light such as speed [1], direction [2], shading of intensity [3], frequency [4] and polarization state [5] to restore three-dimensional shape. For example, a photometric stereo method observes an object from different cameras spaced apart, called a stereo base, while a polarization-based method observes an object in different polarization states by using a polarizer. Naturally by using more lighting parameters, angles, there is more information with which you can restore the shape. In our research we focus on the stereo method and Shape from Polarization to restore the three-dimensional shape.

In this article we want to highlight an important aspect of the 3D scanner - system of calibration. There are many approaches [6] to calibrate a stereo pair, but there are no approaches to calibrate polarization cameras, although this is necessary to achieve accurate results.

In our research were used FLIR BFS-U3-51S5P-C и LUCID PHX050S-PC cameras with similar features as they use the same IMX250MZR matrix Sony CMOS. The cameras have a resolution of 2464 × 2056 and a color depth of 12 bits [7].

II. SHAPE FROM POLARIZATION

The influence of object shape on the polarization of reflected light has been known for centuries and has been formulated in Fresnel equations. This principle is laying in the basis of the "Forms and Polarization" (FIP) methods [8], the purpose of which is a reconstruction of information about the three-dimensional shape of the object on the basis of data on the polarization of light extracted from three or more photographs of the object at different angles of the polarizer.

It is known, that the classical approach to the FIP relies on light reflected specularly from the object. For purpose to use also scattered light as well, Atkinson and Hancock proposed a method which is based solely on the scattered on the object light (here and further named the scattered FIP) [8]. However, the most objects in the real world do not reflect light in exclusively diffused or exclusively mirrored way, but as a composition of these two types of reflection. So as we can see, "mixed reflection" occurs when both the scattered and mirror components reach the camera, what is making the use of FIP techniques quite unusable.

Measuring the surface normals of an object involves a number of problems:

- Knowledge of the refractive index of the object is required.

- It is necessary that the material was either Lambertian one or mirror.

- The azimuth angle of the normal is determined accurate to Pi.

A part of these problems can be solved by using of several algorithms at the same time, which are capable of producing an initial depth map. For example, you can use different algorithms like the Reconstruct Stereo one, Shape from Motion algorithm, Focus-Defocus algorithm, Shape From Shadow algorithm, and etc. Such methods allowed to be led to the practical use of the method.

Fresnel equations are describing the properties of an electromagnetic wave which is reflected by interacting with the surface of an object. At interaction like this two waves are generated– reflected and refracted one. Fresnel equations are relating the parameters of the reflected wave (polarization angle, degree of polarization) with the parameters of the surface material, as well as with the orientation of the normal to the surface.

Form and polarization (FIP) is a term which is used in computer vision for combining a class of methods that are estimating the orientation of object surface normals based on Fresnel equations. Classical FIP is based on measurements of light polarization parameters, which is usually based on three photos with different angles of the polarizer which is mounted on the camera. As we know, there are existing two main directions of FEP: on the basis of reflected mirror light, and also on the basis of scattered light.

The Shape from Polarization algorithm is proposed by the researcher Achuta Kadambi in work [9] and consists of the following stages:

- the computation of the normals map that contains ambiguities for the azimuth angles of normals;

- removing of ambiguity by using a depth map

The polarizer located in front of the camera lens rotates at different angles. The polarizer angles are known in advance and have an exact value. In the used cameras we have 4 angles of rotation equal to 0, 45, 90 and 135 degrees. The intensity of pixels depends on the angle of the polarizer and varies according to the equation that may be written as:

$$I(\Theta_{pol}, \phi) = \frac{I_{max} + I_{min}}{2} + \frac{I_{max} - I_{min}}{2} \cos(2(\Theta_{pol} - \phi)) \qquad (1)$$

Here, θ_{pol} is angle of the polarizer relative to an arbitrary initial value. I_{min} и I_{max} is maximum and minimum pixel intensity when rotating the polarizer. ϕ is the azimuthal angle of the normal to the surface in a spherical coordinate system.

Sampling different values on the sinusoid amounts to taking pictures with different rotations of the polarizer angle.

The azimuthal angle can be calculated by having at least three polarized images. However, there is π ambiguity, since ϕ and $\phi + \pi$ satisfy the intensity change equation.

The degree of polarization which is used to calculate the zenith angle of the normal to the surface is defined as

$$\rho = \frac{I_{max} - I_{min}}{I_{max} + I_{min}} \qquad (2)$$

By using Fresnel equations, the degree of polarization can be represented as follows:

$$\rho = \frac{(n - \frac{1}{n})^2 \sin^2 \Theta}{2 + 2n^2 - (n + \frac{1}{n})^2 \sin^2 \Theta + 4 \cos \Theta \sqrt{n^2 - \sin^2 \Theta}} \qquad (3)$$

where n — the refractive index of the medium and the zenith angle. Knowing the refractive index, the zenith angle can be calculated.

Equation 3 sets forth the degree of polarization for diffuse reflections. Often, refractive index is unknown. But usually dielectrics have refractive index between 1.3 and 1.6. In that range of refractive index, the degree of polarization is not sensitive to the refractive index.

Equation 3 is robust for diffuse reflection from dielectric surfaces, but cannot be used for specular reflection from non-dielectric Surfaces, such as mirrors or metals. For specular reflection from non-dielectric surfaces, the Zenith angle 0 may be calculated using Equation 4:

$$\rho^{spec} = \frac{2n \tan \theta \sin}{\tan^2 \theta \sin^2 \theta + |n^*|^2} \qquad (4)$$

where $|n^*|^2 = n^2(1 + k^2)$, k is the attenuation index of the material, and p is the degree of specular polarization.

To estimate the azimuth of the normal to the surface $\phi 0$, initially the FIP methods used mirror reflection. The maximum value of the reflected light intensity is achieved when the polarizer is aligned with the perpendicularly polarized component of the reflected light, which follows from the Fresnel equations. Atkinson and Hancock [8] showed that for scattered FIP, the maximum is reached for the parallel component, that is, the phase of polarized light shifts by $\pi / 2$ relative to the real azimuth of the normal to the surface, i.e. $\phi = \varphi \pm \pi / 2$.
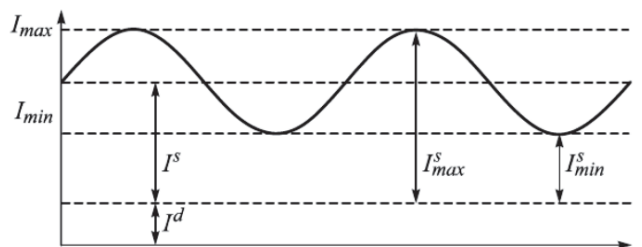
Fig. 1. Intensity of light measured in the chamberdepending on the angle of the polarizer

Two key difficulties in determining the normal azimuth angle:

- Equation (1) contains a cosine with an argument multiplied by 2, which means that with a difference between the phase of polarized light in π there will be no difference in measurements. Thus, the azimuth can

be determined only up to π. This uncertainty is called azimuth uncertainty.

- It is not known a priori whether the light entering the camera is reflected specularly or scattered, so the uncertainty of the azimuth π/2 arises. This uncertainty is called the uncertainty of the reflection model.

II. MATHEMATICS OF POLARIZATION EFFECT.

A physically correct render usually takes into account such things as:

- Fresnel Reflection Coefficients

- Law of energy conservation

- Microfacet theory for reflected light and re-emitted

The list can be expanded on microfacet theory for subsurface scattering and physically correct refraction, etc., but in the context of this article we will talk about the first three points.

In modeling it is allowed an assumption that each surface consists of a set of microsurfaces. Micro-irregularities contribute to the lighting, as their sizes are significantly larger than the wavelength in times, so a rough plane cannot be described by a single normal. Further the normal of macrosurface we will refer to some averaged value of normals of microsurfaces (roughness).
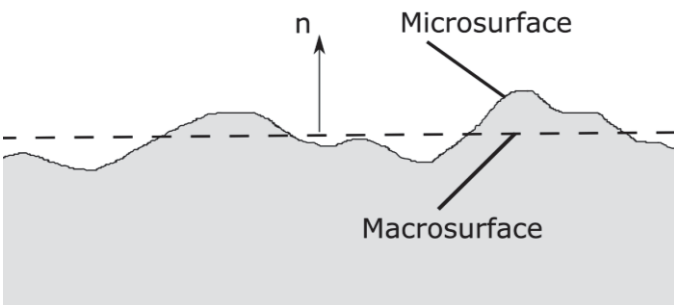
Fig. 2. Micro and macro surfaces

In uneven lighting, it is the microsurfaces that make a significant contribution to the reflected light[10, 11]:

Consider one light source. The light source for simplicity can be considered as a ray or a bundle of rays distributed over a sphere, in both cases, direct rays are reflected from a limited surface area. With a perfectly smooth surface, the rays will hit the camera matrix only if the light source is located at the same angle as the camera (this effect can be observed in the mirror).
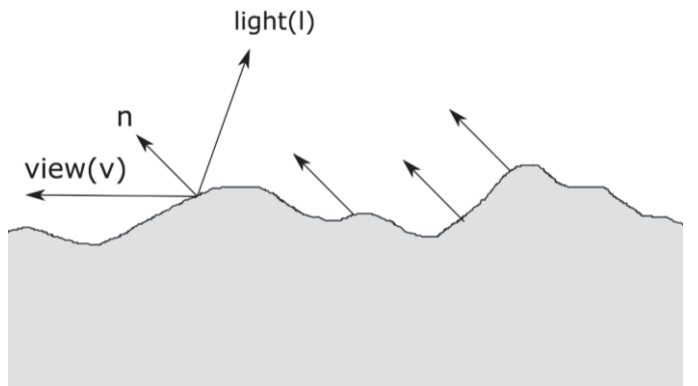
Fig. 3. Light's reflection from microsurfaces
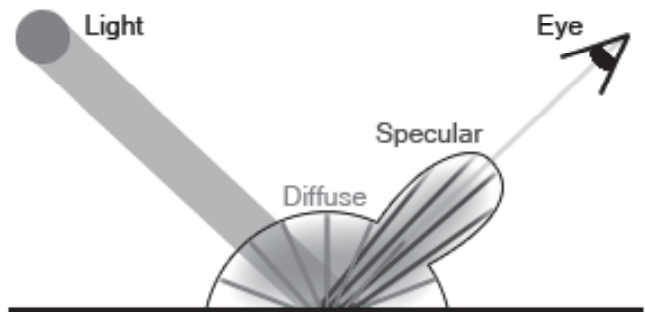
Fig. 4. Diffuse and specular reflection

If the surface is rough, the light is re-reflected and falls on the surfaces are not directly illuminated by the light source. In this case, there are microsurfaces that are not directly illuminated by the light source, but at the same time have an orientation that allows to re-reflect the light into the camera. Geometrically, such surfaces have a normal different from the macro normal, otherwise such surfaces would not be able to re-reflect light in the direction of the camera.
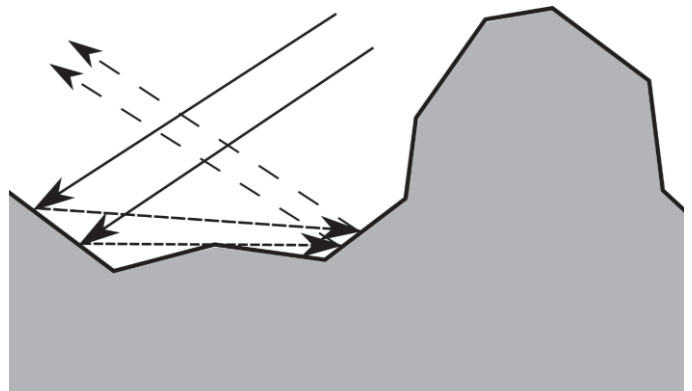
Fig. 5. Re-reflection of light

Consider an example with spheres of different roughness and one light source. In the first image, the roughness of the sphere is minimal, and we see only the rays directly reflected from the surface, such rays will be polarized in the plane of the surface and we can accurately determine its orientation with the increase of roughness re-reflections appear, which we see because there are microsurfaces oriented so that the re-reflected light is directed to the camera.[12, 13] The orientation of such surfaces does not coincide with the orientation of the macrosurface, otherwise the light would be reflected on the principle of "the angle of incidence is equal to the angle of reflection" and we would not see this part of the surface. Accordingly, the light is polarized in the plane of the microsurfaces, and we get the orientation adjusted on re-reflection. Note that at maximum roughness, light depolarizes and we cannot say anything about the orientation of the surface based on polarization.
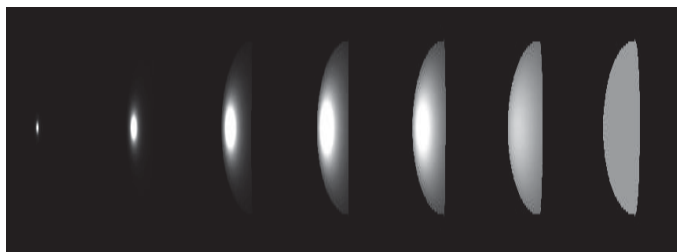
Fig. 6. Specular and diffuse reflection

A ray of light, having hit the border of two different media, is reflected and refracted.
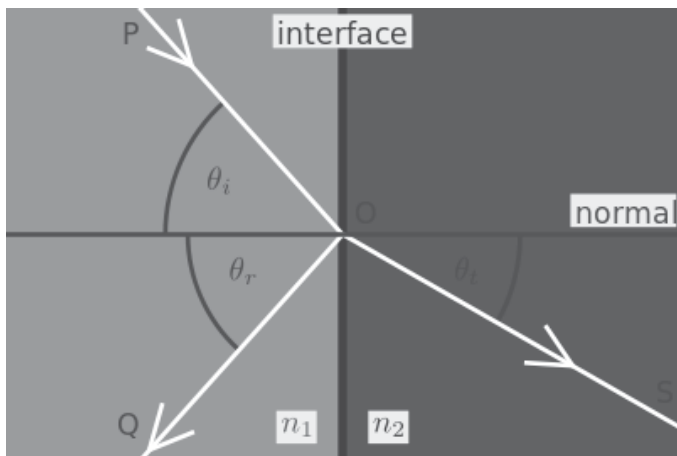
Fig. 7. Specular and diffuse reflection model

Fresnel formulas quite accurately describe the laws by which this happens, but these formulas are quite heavy, but there is a good approximation, which is used in most cases in PBR renders, this is Schlick approximation:

$$R(\theta) = R_0 + (1 - R_0)(1 - \cos \theta)^5$$
$$R_0 = (\frac{n_1 - n_2}{n_1 + n_2})^2 \tag{5}$$

Where R_0 is calculated as the ratio of refractive indices. $\cos\theta$ in the formula is the cosine of the angle between the incidence of light and the normal. It can be seen that for $\cos\theta = 1$, the formula degenerates into R , which means that the physical meaning of R_0 is the amount of reflected light if the beam falls perpendicular to the surface. n_1 and n_2 refraction indexes of surface.

The Cook-Torrance model was used to model the distribution of reflections.

$$k_{spec} = \frac{DFG}{4(V \cdot N)(N \cdot L)} \tag{6}$$

- **V** - vector from the surface to the observer's eye

- **N** - macro-normal of surface

- **L** - direction from surface to light source

- **D** - the function of the distribution of reflected light taking into account micrograins. Describes the number of micrograins turned toward us in way to reflect light into our eyes.

- **G** - function of distribution of self-shadowing and self-concealment. Unfortunately the light re-reflected several times in this function is not taken into account and will be lost. We will return to this point later in the article.

- **F** - Fresnel reflection coefficients. Not all light is reflected. Part of the light is refracted and gets inside the material. In this function, F describes the amount of reflected light.

A microsurface model of physically correct lighting was chosen for the simulation. It is assumed that the surface reflection is due only to the mirror reflection of microsurfaces oriented in the mirror direction relative to the source and the observer. The surrounding space does not take into account in the model that is re-reflections from the walls and surrounding objects are neglected. The model is used to produce a flat image and can be represented for a specific pixel as

$$f_{spec} = \sigma(\theta_i, \theta_s)D(\omega_h)F(\omega_d)F(\phi)G(\omega_i, \omega_s) \tag{7}$$

ω_h — normal of microsurface, ω_d — is the vector of incidence of light in the microsurface's orientation, ω_i — is the vector of incidence of light in the macrosurface's orientation, ω_s — is the vector of observations (of camera) in the macrosurface's orientation.

$$\sigma(\theta_i, \theta_s) = \frac{1}{4\cos(\theta_i)\cos(\theta_s)} \tag{8}$$

The function D is a normal distribution microsurfaces. In the case of isotropic surfaces, the normals of the microsurfaces are uniformly distributed and the distribution depends only on the zenith angle θ_h. Isotropic surfaces are called surfaces whose optical parameters remain unchanged in all directions.

Function G describes the attenuation of light as a result of the dimming of microsurfaces by each other. This model describes the probability of a surface's point being overlapped by another surface/surface's point or the probability of light being re-reflected from multiple microsurfaces and energy loss.

The function F determines the Fresnel reflection for non-polarized incident light. In the classical model, it is a scalar function that describes the amount of reflected light. In general case, F is a 4×4 Muller matrix. $F(\omega_d)$ — is Mueller matrix for Fresnel reflection, $F(\phi)$ — is Mueller matrix for linear polarizer at an angle ϕ.

$$F(\omega_d) = \frac{1}{2}\left(\frac{\tan\alpha_-}{\tan\alpha_+}\right)^2 \times$$
$$\times \begin{bmatrix} \cos^2\alpha_- + \cos^2\alpha_+| & \cos^2\alpha_- - \cos^2\alpha_+ & 0 & 0 \\ \cos^2\alpha_- - \cos^2\alpha_+ & \cos^2\alpha_- + \cos^2\alpha_+ & 0 & 0 \\ 0 & 0 & -2\cos\alpha_-\cos\alpha_+ & 0 \\ 0 & 0 & 0 & -2\cos\alpha_-\cos\alpha_+ \end{bmatrix} \quad (9)$$

where $\alpha_\pm = d\pm t$ — is the sum/difference of the angle of incidence and refraction. For the transition from $cos(\theta_t)$ to $cos(\theta_d)$ Snell's law is used: $sin(\theta_t) = n1/n2\ sin(\theta_d)$.

$$F(\phi) = \frac{1}{2}\begin{bmatrix} 1 & \cos 2\phi & \sin 2\phi & 0 \\ \cos 2\phi & \cos^2 2\phi & \sin 2\phi\cos 2\phi & 0 \\ \sin 2\phi & \sin 2\phi\cos 2\phi & \sin^2 2\phi & 0 \\ 0 & 0 & 0 & 0 \end{bmatrix} \quad (10)$$

III. MODELING AND COMPARISON WITH REAL DATA

In the simulation, the plane is considered, the azimuthal angles of the normals to each point of the plane are the same and equal to zero. The resulting normal map is shown below in the graph, the spread reaches 80 degrees.
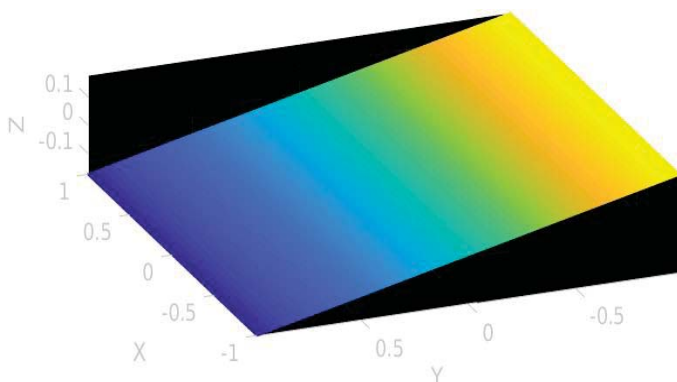
Fig. 8. A cloud of plane's points with an azimuthal angle of 0
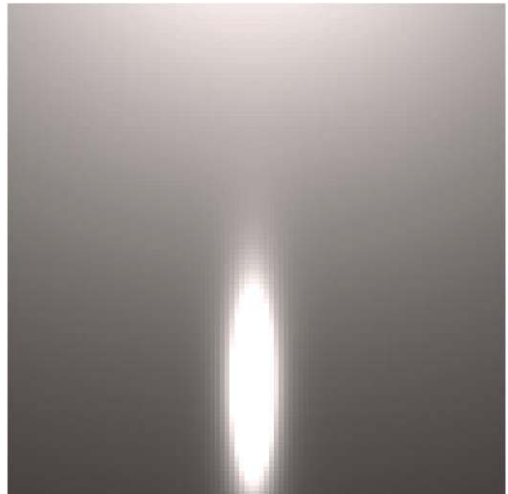
Fig. 9. Projection on the camera matrix
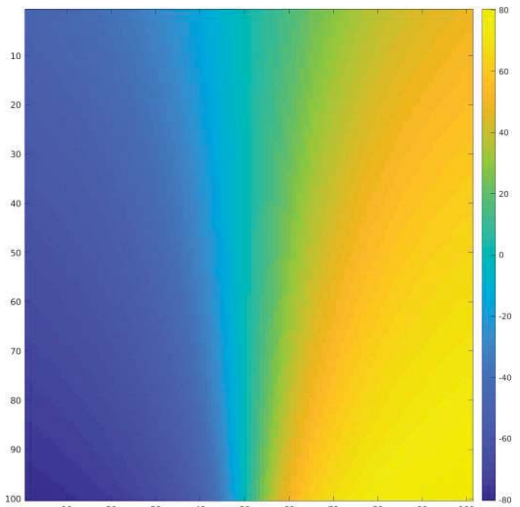
Fig. 10. Map of the azimuthal angles of the surface that was resulted

You can see that when using the SFP algorithm, the azimuth angles map varies from -80 to 80 degrees. Thus, when restoring the 3D surface, we must obtain the same map of normals, what is confirmed by theoretical calculations. This is explained by the geometric location of the light source and the location of the camera. When shooting in real conditions, a similar "gradient" of azimuthal angles on a flat surface is obtained.
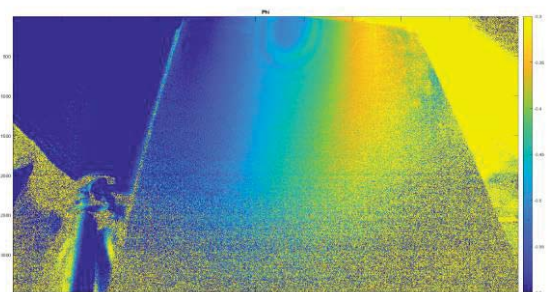
Fig. 11. Map of azimuthal angles of the plane in real conditions

In this figure, the azimuthal angles vary from 16 to 35 degrees. This effect for the correct 3D reconstruction of the surface can be reduced by removing the camera and the light source from each other and from the object under study

In the simulation, three experiments will be conducted on the dependence of the azimuthal angle's error from the distance of the camera and the light source from each other. There are shown the images on camera's matrix of the flat surface.
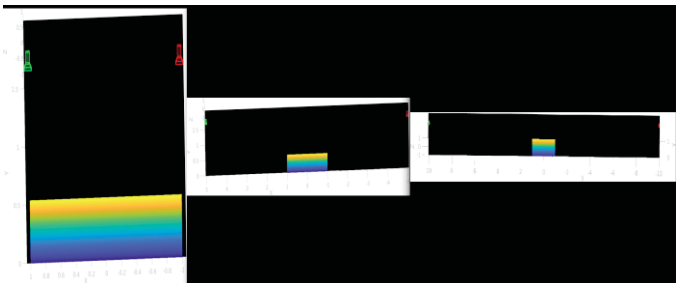
Fig. 12. Geometric arrangement of the camera and light source
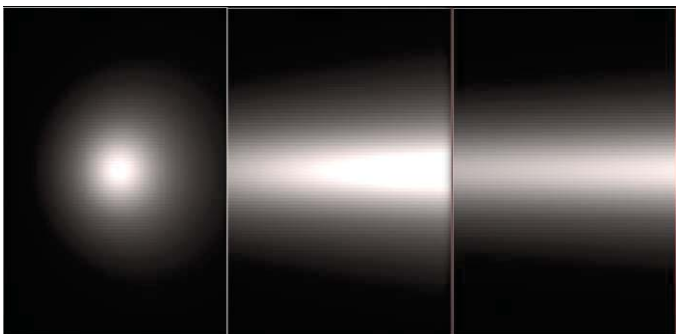
Fig. 13. Image obtained on the camera matrix
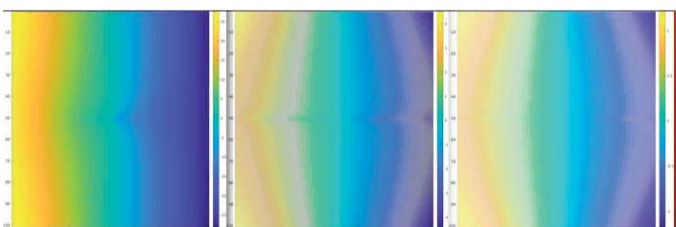
Fig. 14. Azimuthal angles of three experiments

As you can see that with increasing distance the error of the azimuthal angle decreases, and at the last experiment the error was equal to 1 degree, the first experience to 100 degrees. More accurate measurements should be made by taking into account the physical parameters of the camera and the environment, what can be considered when calibrating the camera.

IV. CONCLUSION

The article examined the Shape From Polarization algorithm and developed a mathematical apparatus for modeling that allows you to set the physical characteristics of the surface, based on Physically Based Rendering. Assessments were made of the accuracy of obtaining the surface shape of objects at different distances from the light source and the camera, and comparisons were made with real results obtained under conditions close to the simulation. For a more accurate calculation, it is necessary to take into account the geometric arrangement of the light source and the camera, have accurate data on the type of the surface under study, calculate its coefficients and enter into the mathematical model of the system. Such a method will help to calculate the error of obtaining an accurate depth map using the Shape From Polarization algorithm, will allow you to pre-calculate the necessary characteristics of a 3D scanner, such as lens characteristics, matrix size, physical dimensions of the scanner body, etc.

For more accurate modeling, it is possible to introduce taking into account additional physical effects of rereflection, microfacet theory for subsurface scattering and physically correct refraction, Anisotropic Lighting Models, Subsurface Scattering, Advanced Diffuse Lighting Models such as Oren-Nayar, Capture Spherical Harmonics, Capture Tonmapping etc.

REFERENCES

[1] *S. Foix and G. Aleny. Lock-in Time-of-Flight (ToF) Cameras : A Survey. IEEE Sensors Journal, 11(3):1–11, 2011.*

[2] *Robert J. Woodham. Photometric Method For Determining Surface Orientation From Multiple Images. Optical Engineering, 19(1), 1980.*

[3] *I. Sato, T. Okabe, Q. Yu, and Y. Sato. Shape Reconstruction Based on Similarity in Radiance Changes under Varying Illumination. 2007 IEEE 11th International Conference on Computer Vision, pages 1–8, 2007.*

[4] *C. P. Huynh, A. Robles-Kelly, and E. R. Hancock. Shape and Refractive Index from Single-View Spectro-Polarimetric Images. International Journal of Computer Vision, 101(1):64– 94, June 2013.*

[5] *G. A. Atkinson and E. R. Hancock. Surface Reconstruction Using Polarization and Photometric Stereo. Computer Analysis of Images and Patterns Lecture Notes in Computer Science, pages 466–473, 2007.*

[6] *O. Drbohlav and R. Sara. Unambiguous determination of shape from photometric stereo with unknown light sources. In ICCV, pages 581–586, 2001.*

[7] *Polarization Image Sensor, https://www.sony-semicon.co.jp/products_en/IS/sensor5/index.html [viewing date: 09.04.2019].*

[8] *Atkinson GA, Hancock ER.* Recovery of surface orientation from diffuse polarization. IEEE Transactions on Image Processing 2006; 15(6): 1653-1664.

[9] *Achuta Kadambi и Vage Taamazyan и Boxin Shi и Ramesh Raskar. Polarized 3d: High-quality depth sensing with polarization cues. Технический отчёт, MIT Media Lab, 2015.*

[10] O. Drbohlav and R. Šára. Specularities reduce ambiguity of uncalibrated photometric stereo. In Proc. ECCV, pages 46–62, 2002.Cula OG, Dana KJ, Pai DK, Wang D. Polarization multiplexing and demultiplexing for appearance-based modeling. IEEE Trans Pattern Anal Mach Intell 2007; 29(2): 362-367.

[11] Rahmann S, Canterakis N. Reconstruction of specular surfaces using polarization imaging. Proceedings of the 2001 IEEE Computer Society Conference on Computer Vision and Pattern Recognition (CVPR 2001) 2001; 1: I–149-I–155.

[12] Lin, S., Shum, H.Y.: Separation of diffuse and specular reflection in color images. In: Proceedings of the 2001 IEEE.Computer Society Conference on Computer Vision and Pattern Recognition (CVPR 2001) 2001; 1: I–341-I–346.

[13] Izadi S, Kim D, Hilliges O, Molyneaux D, Newcombe R, Kohli P, Shotton J, Hodges S, Freeman D, Davison A, Fitzgibbon A. Kinectfusion: Real-time 3D reconstruction and interaction using a moving depth camera. UIST '11 Proceedings of the 24th annual ACM symposium on User interface software and technology 2011: 559-568.